NANO LETTERS

2007
Vol. 7, No. 8
2486−2490

III–V Nanowire Growth Mechanism: V/III Ratio and Temperature Effects

Shadi A. Dayeh, Edward T. Yu,* and Deli Wang*

Department of Electrical and Computer Engineering, University of California−San Diego, La Jolla, California 92093

Received May 29, 2007

ABSTRACT

We have studied the dependence of Au-assisted InAs nanowire (NW) growth on InAs(111)B substrates as a function of substrate temperature and input V/III precursor ratio using organometallic vapor-phase epitaxy. Temperature-dependent growth was observed within certain temperature windows that are highly dependent on input V/III ratios. This dependence was found to be a direct consequence of the drop in NW nucleation and growth rate with increasing V/III ratio at a constant growth temperature due to depletion of indium at the NW growth sites. The growth rate was found to be determined by the local V/III ratio, which is dependent on the input precursor flow rates, growth temperature, and substrate decomposition. These studies advance understanding of the key processes involved in III–V NW growth, support the general validity of the vapor–liquid–solid growth mechanism for III–V NWs, and improve rational control over their growth morphology.

III−V compound semiconductor nanowires (NWs) can be synthesized using a variety of growth techniques including organometallic vapor-phase epitaxy (OMVPE),[1−3] molecular[4] and chemical[5] beam epitaxy, wafer annealing,[6] chemical vapor deposition,[7] laser ablation,[8,9] and low-temperature solution methods.[10] However, the detailed mechanisms for NW growth that apply for different growth techniques and conditions remain an active subject of investigation and debate. In the presence of catalytic metal particles, NW growth evolution is interpreted as occurring via the vapor−liquid−solid (VLS)[1,4−8] and vapor−solid−solid (VSS)[2] growth mechanisms. In the absence of metal particles, their growth is interpreted via group-III catalyzed VLS growth,[3,11,12] oxide-assisted growth,[9] ligand-aided solution−solid (LSS) growth,[10] and, more recently, reactive Si-assisted growth.[13]

Growth from a solid particle, that is, the VSS mechanism, was first proposed in 1979 for Ag-catalyzed Si whiskers[14] and, more recently, for Ti-catalyzed[15] and Al-catalyzed[16] Si NWs that were grown at temperatures much lower than the eutectic melting temperatures of Ag−Si, Ti−Si, or Al−Si alloys. Using similar arguments, this growth mechanism was invoked for III−V NWs,[2,17] as well as to explain the cessation of Au-assisted InAs NW growth on an InAs (111)B substrate at temperatures thought to be the Au−In tip alloy melting temperatures.[18] In the latter report, a passivation layer of SiO_x allowed growth at much higher temperatures, which was attributed to lower In incorporation into the Au nanoparticle.

In this paper, we show that the input V/III ratio together with the substrate temperature determine the NW nucleation and growth rate, and, consequently, the temperature at which cessation of III−V NW growth occurs. Higher V/III ratios were found to favor vapor−solid (VS) surface growth over VLS NW growth. By tuning both the group III flow rate and the growth temperature, control over NW morphology is enabled. These experimental findings provide significant new insight into the diverse growth behavior observed in a number of other III−V growth reports.[2,17,18]

The growth experiments reported in this paper were performed in a horizontal OMVPE growth tube using trimethylindium and arsine precursors in 1.2 L/min H_2 carrier gas and at a chamber pressure of 100 Torr. Au nanoparticles 40 nm in diameter were dispersed at a density of $\sim 0.3/\mu m^2$ on InAs(111)B substrates precoated with poly-L-lysine, followed by UV ozone cleaning at 100 °C for 5 min. AsH_3 flow was maintained in the chamber throughout the entire growth process including temperature ramp up and cool down, while TMIn was introduced for 6 min after reaching the desired growth temperature. The V/III ratio was changed by both altering the AsH_3 flow rate at a fixed TMIn flow and vice versa.

We first studied the temperature-dependent InAs NW growth rate on InAs(111)B substrates by fixing the input V/III ratio at 60 with a TMIn flow rate of 0.75 μmol/min, and varying the substrate temperature in the range of 425−525 °C. Figure 1a−d shows 45° angle field emission scanning electron microscope (FE-SEM) images of the resulting InAs NWs grown at different temperatures, taken from the center of InAs (111)B samples of similar area for consistency in comparison. The NW growth rate increases as the temperature increases up to ∼475 °C, after which the

* Corresponding author. E-mail: ety@ece.ucsd.edu (E.T.Y.); dwang@ece.ucsd.edu (D.W.).

10.1021/nl0712668 CCC: $37.00
Published on Web 07/04/2007

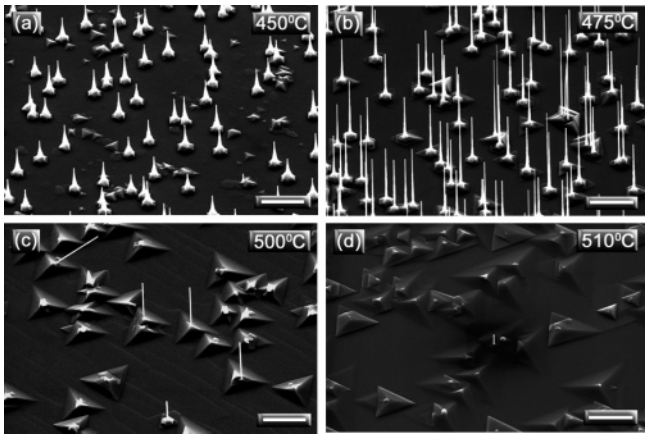

Figure 1. Growth of InAs NWs on InAs(111)B at a constant V/III ratio of 60 and different growth temperatures. Scale bars are 2 μm.

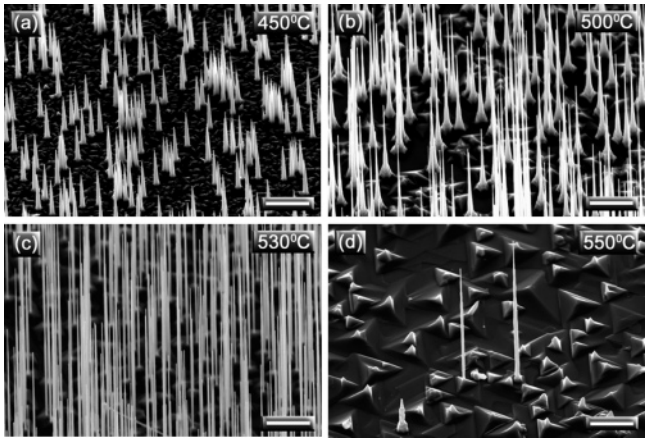

Figure 2. Growth of InAs NWs on InAs(111)B at a constant V/III ratio of 7.5 and different growth temperatures. Scale bars are 2 μm.

NW growth rate drops. No NW growth was observed at a temperature of 525 °C. This is consistent with earlier growth reports on the temperature dependence of InAs NW growth.[2,18] However, as the input V/III ratio is altered, the NW growth exhibits a different cessation temperature. Figure 2a−d shows 45° FE-SEM images of InAs NWs grown in the temperature range of 425−560 °C with a TMIn flow rate of 6 μmol/min (input V/III = 7.5). Growth at the same temperature and a lower V/III ratio leads to longer NWs with higher density. NW growth persists up to at least 560 °C, which is higher than the temperature at which NW growth rate drops sharply at an input V/III ratio of 60.

Figure 3 shows the temperature-dependent growth rate calculated for the two sets of growth experiments described above. Although the NW growth rate should take into account the NW growth density and volume,[19] here only the NW lengths are considered for consistent comparison with other growth reports.[2,18] For the two studied input V/III ratios, the NW length increases with temperature due to the lowered energy barriers and increased surface In adatom mobility. At a V/III ratio of 60, the InAs NW growth rates and the temperature (∼510 °C) at which the NW growth ceases are very similar to those reported in a similar growth experiment performed at a V/III ratio of 67.[18] However, we observe that

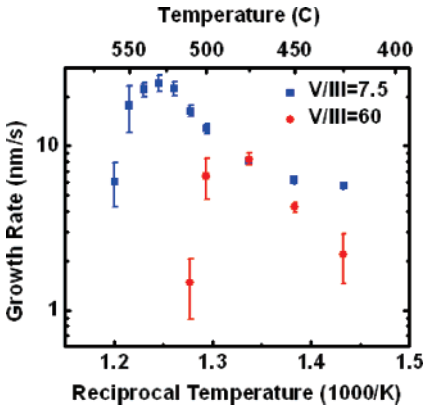

Figure 3. Temperature-dependent growth rate of InAs NWs on InAs(111)B substrates for two different V/III ratios. Red dots are obtained at a TMIn flow rate of 0.75 μmol/min (V/III = 60) and blue squares were obtained at an input flow rate of 6 μmol/min (V/III = 7.5).

the NW growth rate drops sharply at about 560 °C at an input V/III ratio of 7.5, which is ∼50 °C higher than that for a V/III ratio of 60. These results demonstrate that the input V/III ratios strongly influence the temperature dependence of NW growth and cessation, in contrast to what has been postulated previously.[18]

To elaborate on the dependence of growth rate on the input V/III ratio, we performed a set of experiments at 500 °C and varied the input V/III ratio. Figure 4 shows FE-SEM images of InAs NWs grown on InAs(111)B at T = 500 °C, and with a constant TMIn flow rate of 0.97 μmol/min and different AsH_3 flow rates. For V/III ratios of 92 (Figure 4a) and 150 (not shown), no NW growth was observed at the center of the sample. It is known that the activation energy for the heterogeneous reactions at the growth interface (which are dependent on precursor pyrolysis) decreases as the input V/III ratio is increased.[20] Thus, the mobility of available In on the substrate surface is reduced due to crystallization on the substrate surface rather than at the NW growth site at its tip. Due to the resulting depletion of In from the NW growth sites, the NW nucleation rate drops as the effective V/III ratio is increased. Thus, VS or thin film growth is expected to be favored over VLS growth as the V/III ratio is increased. The inset of Figure 4a shows a cross-sectional FE-SEM image with InAs islands formed under Au nanoparticles but with no NW growth. The enhanced surface growth under the Au nanoparticle is due to more efficient AsH_3 pyrolysis in the nanoparticle vicinity and, consequently, the more favored surface growth. As the V/III ratio is reduced to 68 (Figure 4b), InAs NWs grow, but at a relatively small density of NW/Au nanoparticles (∼3%). At a V/III ratio of 45 (Figure 4c), more efficient NW growth is obtained (∼50% NW/Au nanoparticle), and the average NW length is slightly increased. Further reduction in the V/III ratio is limited by the accuracy of the AsH_3 mass flow controllers in our OMVPE system. Note that, at high V/III ratios, some NWs grow at an angle with respect to the substrate normal (Figure 4b).

On the other hand, for a fixed AsH_3 flow rate of 44.6 μmol/min, the NW growth rate and density are reduced as the input

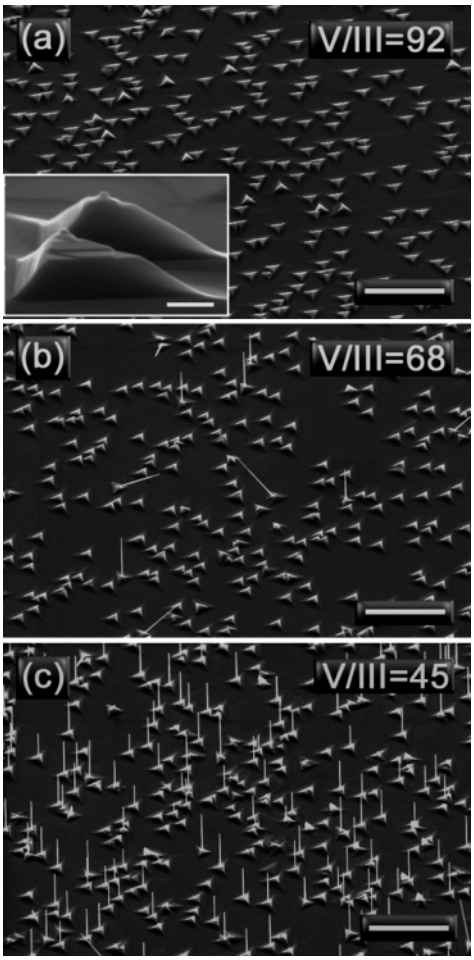

Figure 4. 45° FE-SEM images of InAs NWs grown at 500 °C and different input V/III ratios. Scale bars are 5 μm. Inset of panel a is a cross-sectional view of two islands showing surface growth with Au nanoparticles atop the islands. Inset scale bar is 200 nm.

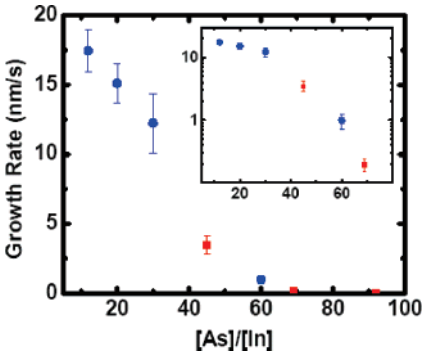

Figure 5. Input V/III ratio-dependent growth rate of InAs NWs on InAs(111)B at a growth temperature of 500 °C. Inset is the same growth rate plotted in log scale. Blue circles were obtained at a fixed AsH_3 flow rate of 44.6 μmol/min, and the red squares were obtained at a fixed TMIn flow rate of 0.97 μmol/min.

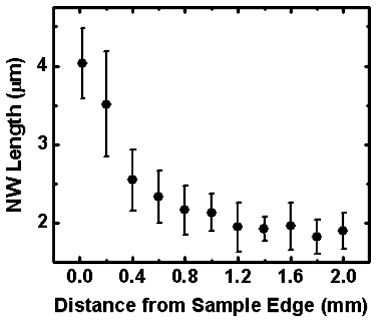

Figure 6. Variation of the NW length as a function of distance from the sample edge grown at 500 °C and input V/III = 149 (TMIn = 0.9 μmol/min and AsH_3 = 134 μmol/min).

V/III ratio is increased due to the direct dependence of the growth rate on group III flow for V/III ratios greater than 1.[12] Specifically, at a V/III ratio of 60 corresponding to a TMIn flow rate of 0.75 μmol/min, the growth density was ~15% NW/Au nanoparticles, whereas for very low V/III ratios (<10) corresponding to TMIn flow rates greater than 4.7μmol/min, multiple NWs per single InAs island can grow.[12] Figure 5 shows a plot of the NW growth rate as a function of the input V/III ratio obtained by changing either AsH_3 or TMIn precursor flow rates, demonstrating reduction in the effective NW growth rate as the input V/III ratio increases. The NW growth rate ρ was calculated using $\rho = (L/t)(N/M)$, where L is the average NW length, t is the growth time, and N/M is the growth density of NW/Au nanoparticles where N is the number of NWs and M is the number of InAs islands formed around the Au nanoparticles, both calculated in constant area. Note from Figure 5 that the NW growth rates are dependent on the V/III ratio when either TMIn or AsH_3 are varied. However, the NW growth rate shows a stronger dependence on changing TMIn flow, not only because the V/III ratio is changed, but also because of the direct dependence of the growth rate on group III flow for V/III $\geq$ 1.[12] From the inset of Figure 5, we can observe that, at high V/III ratios, the NW growth rate drops similarly as both TMIn or AsH_3 flow rates are changed, whereas, at low V/III ratios (high TMIn flow), the NW growth rate follows a different and larger slope dictated by the change in TMIn flow.

The growth rate dependence on V/III ratio can be clearly seen on an inert surface of different atomic constituents than the grown material. For example, on SiO_2/Si surfaces, NW growth is favored at a low input V/III ratio with little island growth on the substrate surface. As the input V/III ratio is increased, the NW length, diameter, and growth density decrease until NW growth ceases and the InAs two-dimensional growth density on the SiO_2 surface increases (see Supporting Information for experiments on SiO_2 surfaces at different V/III ratios).

We also observe that the NW growth rate is relatively constant across the growth substrate for a low input V/III ratio, that is, when the growth rate is high. However, variations in the growth rate from the center toward the edges of the substrate become apparent as the input V/III ratio or temperature increases. Figure 6 shows variation in the NW lengths as a function of distance from the substrate edge at an input V/III ratio of 150 and a growth temperature of 500 °C. The growth density decreases as the distance from the sample edge increases until no NW growth was observed at a distance of 2.4 mm. This is similar to what we observed for the growths at 510 °C with a V/III ratio of 60 and at 550 °C with a V/III ratio of 7.5, where little to no NW growth was observed at the center of the substrates (~1 × 1 cm^2),

as seen in Figures 1d and 2d, respectively. NW growth prevails toward the substrate edges with higher growth density, growth rate, and different morphology. Such behaviors are commonly referred to as "edge" effects where precursor pyrolysis and barrier layers may differ at the edge from those at the center of the substrate. Because Au nanoparticles enhance AsH_3 pyrolysis[19] and decomposition of the InAs substrate at high temperatures (see Supporting Information, Figure S3), the local V/III ratio is thus expected to vary over the substrate surface. This effect is thus maximal at the substrate center compared to its edges. We believe that substrate decomposition and the subsequent alteration of the V/III ratio leads to such variation in the NW growth rate across the sample.

The effective V/III ratio during growth depends not only on the input precursor molar fraction but also the growth temperature. As the temperature is increased, AsH_3 pyrolysis is also increased, resulting in a higher effective local V/III ratio, which favors VS growth over VLS growth. Consequently, the NW growth rate drops, and eventually the NW growth ceases. More specifically, at a lower input V/III ratio (V/III = 7.5) with less group V in the vapor, higher temperatures are required to pyrolyze AsH_3 and create a high enough local V/III ratio to cease the NW growth, when compared to a higher input V/III ratio (V/III = 60). This precisely describes the NW growth rate behavior in Figure 3.

Indeed, the slight difference reported previously in the cessation temperature (490 °C vs 460 °C) for NW growth on InAs(111)B surfaces subjected to different pregrowth annealing treatments was attributed to differences in In content in the Au−In alloy particle at the NW tip,[18] as a higher In content would imply a lower melting temperature from the Au−In phase diagram. A close examination of the same growth report, however, shows that input V/III ratios of 67 and 83 resulted in NW growth cessation at 490 and 460 °C, respectively, in good agreement with our postulate of the NW growth rate dependence on the input V/III ratio. Therefore, we attribute the difference in the growth rate and cessation temperature to the variation in the input V/III ratio, and not to the difference in the melting temperatures of the Au−In particle alloy at the tip of the NW. In a related study of NWs that were grown on InAs(111)B substrates covered with SiO_x, the contribution of the substrate in altering the effective V/III ratio is likely to be reduced by the capping SiO_x, which also may allow longer surface diffusion lengths of In adatoms than on the InAs(111)B surface. As a result, In may not be easily depleted from the NW growth sites due to crystallization on the SiO_x surface, and the NW growth would consequently prevail to temperatures higher than those on InAs(111)B surfaces. Thus, we conclude from our studies and analysis of related results that experimental observations of NW growth cessation at different growth temperatures do not necessarily constitute evidence for the VSS growth mechanism for III−V NWs.[2,18] Moreover, it has been shown that, when the growth substrate is cooled rapidly in a water bath immediately after growth, thus minimizing In diffusion from the growth globule,[21] the presence of substantial In in the Au nanoparticle suggested growth via the VLS mechanism.[7,22] Furthermore, recent in situ transmission electron microscope studies on Au-catalyzed Ge NW growth have shown hysteresis in the solid−liquid phase transformation with temperature.[23] These studies suggest that post-growth compositional[18] and phase analyses[17] at the tip of the NW are not necessarily definitive in determining the possibility of growth from a solid seed.

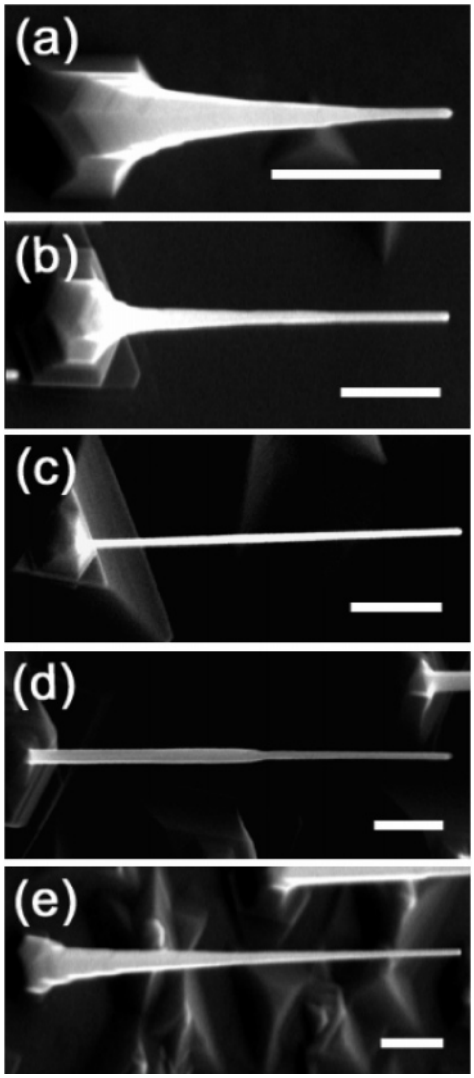

Figure 7. 45° FE-SEM images of InAs NWs grown at (a) 450 °C, (b) 475 °C, and (c) 500 °C with constant TMIn and AsH_3 molar flow rates of 0.75 and 44.6 μmol/min, respectively (V/III = 60). Also shown are FE-SEM images of InAs NWs grown at 500 °C and different TMIn molar flow rates of (d) 1.5 μmol/min and (e) 2.25 μmol/min. Scale bars are 500 nm.

These studies not only enable understanding of the III−V NW growth mechanism, but also allow control over their morphology. Figure 7a−c shows FE-SEM images of InAs NWs grown at a constant input V/III ratio (60) and different growth temperatures. As the growth temperature is increased, the mobility of In adatoms on the surface of the NW is increased, which enables them to reach the growth tip. Thus, tapering, which is observed at 450 °C (Figure 7a) and 475 °C (Figure 7b), is diminished at 500 °C (Figure 7c). At a constant growth temperature of 500 °C, if the input TMIn

flow rate is increased, more In is available at the surface of the NW, and tapering increases, as shown in Figure 7d,e.

In summary, we have shown that OMVPE growth of InAs NWs occurs within certain temperature windows, where NW nucleation and growth increase with increase in temperature, reach maxima, then decrease, and stop. The temperature window within which NWs grow depends on the input V/III ratio, and both the growth temperature and the V/III input ratio determine the NW growth rate and morphology. At a constant temperature, higher V/III input ratio results in higher surface growth rates and reduced NW growth rates. For a constant V/III ratio, III−V NWs grow in the kinetically limited growth regime up to temperatures at which the local V/III ratio is enhanced due to efficient hydride pyrolysis, and thus the NW growth rate starts to drop. These results help in explaining different III−V NW growth behavior obtained from different growth techniques, support the general validity of the VLS growth mechanism for III−V NWs, and facilitate control over their growth morphology.

Acknowledgment. We thank Prof. Paul K. L. Yu for providing access to the OMVPE facility in which the growth experiments were performed. We would like to acknowledge the financial support from the Office of Naval Research (ONR-nanoelectronics), the National Science Foundation (ECS-0506902), and Sharp Labs of America. S.A.D. is grateful for the W. S. C. Chang's fellowship support during the period of this study.

Supporting Information Available: Details of InAs NW growth experiments on SiO_2/Si surfaces at different V/III ratios. This material is available free of charge via the Internet at http://pubs.acs.org.

References

(1) Yazawa, M.; Koguchi, M.; Muto, A.; Jiruma, K. *Adv. Mater.* **1993**, *5*, 577.
(2) Dick, K. A; Deppert, K; Karlsson, L. S.; Wallenberg, L. R.; Samuelson, L; Seifert, W. *Adv. Funct. Mater.* **2005**, *15*, 1603.
(3) Novotny, C. J.; Yu, P. K. L. *Appl. Phys. Lett.* **2005**, *87*, 203111.
(4) Dubrovskii, V. G.; Cirlin, G. E.; Soshnikov, I. P.; Tonkikh, A. A.; Sibirev, N. V.; Samsonenko, Y. B.; Ustinov, V. M. *Phys. Rev. B* **2005**, *71*, 205325.
(5) Jensen, L. E.; Björk, M. T.; Jeppesen, S.; Persson, A. I.; Ohlsson, B. J.; Samuelson, L. *Nano Lett.* **2004**, *4*, 1961.
(6) Zhi, C. Y.; Bai, X. D.; Wang, E. G. *Appl. Phys. Lett.* **2004**, *85*, 1802.
(7) Park, H. D.; Prokes, S. M.; Cammarata, R. C. *Appl. Phys. Lett.* **2005**, *87*, 063110.
(8) Duan, X.; Wang, J.; Lieber, C. M. *Appl. Phys. Lett.* **2000**, *76*, 1116.
(9) Shi, W. S.; Zheng, Y. F.; Wang, N.; Lee, C. S.; Lee, S. T *Appl. Phys. Lett.* **2001**, *78*, 3304.
(10) Xu, X.; Wei, W.; Qiu, X.; Yu, K.; Yu, R.; Si, S.; Xu, G.; Huang, W.; Peng, B. *Nanotechnology* **2006**, *17*, 3416.
(11) Kasahara, J.; Kajiwara, K.; Yamada, T. *J. Cryst. Growth* **1977**, *38*, 23.
(12) Dayeh, S. A.; Yu, E. T.; Wang, D. *Small*, in press.
(13) Park, H. D.; Prokes, S. M.; Twig, M. E.; Cammarata, R. C.; Gaillot, A.-C. *Appl. Phys. Lett.* **2006**, *89*, 223125.
(14) Tatsumi, Y.; Hirata, M.; Shigi, M. *Japan. J. Appl. Phys.* **1979**, *18*, 2199.
(15) Kamins, T. I.; Williams, R. S.; Basile, D. P.; Hesjedal, T.; Harris, J. S. *J. Appl. Phys.* **2001**, *89*, 1008.
(16) Wang, Y.; Schmidt, V.; Senz, S.; Gösele, E. *Nat. Nanotechnol.* **2006**, *1*, 186.
(17) Persson, A. I.; Larsson, M. W.; Stenström, S.; Ohlsson, B. J.; Samuelson, L.; Wallenberg, L. R. *Nat. Mater.* **2004**, *3*, 677.
(18) Dick, K. A.; Deppert, K.; Martensson, T.; Mandl, B.; Samuelson, L.; Seifert, W. *Nano Lett.* **2005**, *5*, 761.
(19) Dayeh, S. A.; Yu, E. T.; Wang, D. *J. Phys. Chem. C*, submitted for publication, 2007.
(20) Reep, D. J.; Ghandi, S. K. *J. Electrochem. Soc.* **1984**, *131*, 2697.
(21) Hasumi, Y. *J. Appl. Phys.* **1985**, *8*, 3081.
(22) Park, H. D.; Gaillot, A.-C.; Prokes, S. M.; Cammarata, R. C. *J. Cryst. Growth* **2006**, *296*, 159.
(23) Kodambaka, S.; Tersoff, J.; Reuter, M. C.; Ross, F. M. *Science* **2007**, *316*, 729.

NL0712668